JACS
JOURNAL OF THE AMERICAN CHEMICAL SOCIETY
pubs.acs.org/JACS
Article

Bioorthogonal Photoreactive Surfaces for Single-Cell Analysis of Intercellular Communications

Takahiro Kosaka, Satoshi Yamaguchi,* Shin Izuta, Shinya Yamahira, Yoshikazu Shibasaki, Hiroaki Tateno, and Akimitsu Okamoto*

Cite This: https://doi.org/10.1021/jacs.2c07321
Read Online
ACCESS | Metrics & More | Article Recommendations | Supporting Information

ABSTRACT: Methods to construct single-cell pairs of heterogeneous cells attract attention because of their potential in cell biological and medical applications for analyzing individual intercellular communications such as immune and nerve synaptic interactions. Photoactivatable substrate surfaces for cell anchoring are promising tools to achieve single-cell pairing. However, conventional surfaces that photoactivate a single type of cell anchoring moiety restrict the combination of cell pair types and their applications. We developed a photoresponsive material comprising a bioorthogonal photoreactive moiety and non-cell adhesive hydrophilic polymer. The material-coated surface allows conjugation with various cell anchoring molecules in response to light at specific timings and consequently achieves light-induced anchoring of a variety of cells at defined regions. Using the platform surface, an array of cancer cell and natural-killer (NK) cell pairs was constructed on a flat substrate surface and the dynamic morphological changes of the cancer cells were monitored by cytotoxic interaction with NK cells at a single-cell level. The photoreactive surface is a useful tool for image-based investigation of the communications between a variety of cell types.

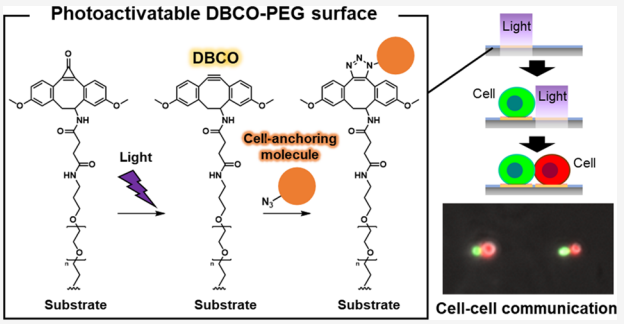

INTRODUCTION

As more attention is given to the importance of cellular heterogeneity in cell biology, pharmacology, and medicine, techniques are needed to evaluate cell functions at the single-cell level.[1−3] Intercellular communications via interactions between the receptor and ligand proteins play essential roles in regulating cellular functions in a variety of biological systems.[4,5] Therefore, single-cell analysis of intercellular communications is expected to provide new insight in drug discovery, diagnosis, and therapy that cannot be clarified by conventional analysis using the average of a cell population. Toward this goal, methods for preparing a large number of heterogeneous cell pairs are critical for observing their communications in a high-throughput manner. So far, such methods using microelectromechanical systems (MEMS) have been reported.[6−13] Dura *et al.* achieved single-cell pairing of lymphocytes in a microfluidic device with microstructures for cell trapping, leading to high-throughput profiling of the interactions between different lymphocytes.[6,7] Sarker *et al.* reported a method to confine an immune cell and cancer cell in a microdroplet and observed their cytotoxic interaction.[11,12] In this study, we envisioned the use of a photoresponsive material for light-induced anchoring of pairs of heterogeneous cells on a flat culture substrate without microstructures for cell trapping. In principle, on photoresponsive surfaces, the cell anchoring areas can be dynamically and freely created by exposure to light with high resolution at a single-cell level. As a result, cell pairs can be constructed by anchoring the second cell at the position neighboring the first anchored cell at a specific time during culture of the first cell (Figure 1).

Light-guided cell adhesive surfaces based on photoresponsive materials have been studied extensively.[14−17] In a pioneering study, Nakanishi *et al.* demonstrated single-cell analysis using their photoactivatable cell adhesive surfaces with light-induced desired cell positions.[14] However, the existing photoactivatable surfaces based on cell adhesion can only be applied to adherent cells. Therefore, they are not applicable for the single-cell analysis of the intercellular communications involving non-adherent or weakly adherent cells, which include immunocytes and some cancer cells. Additionally, in most cases, it takes more than a few hours to attach each cell to defined positions. In cell pairing on such surfaces, it is difficult to attach the second cell before the first cell moves from the defined position. Additionally, the starting time of intercellular communications cannot be accurately defined because the communications start

Received: July 11, 2022

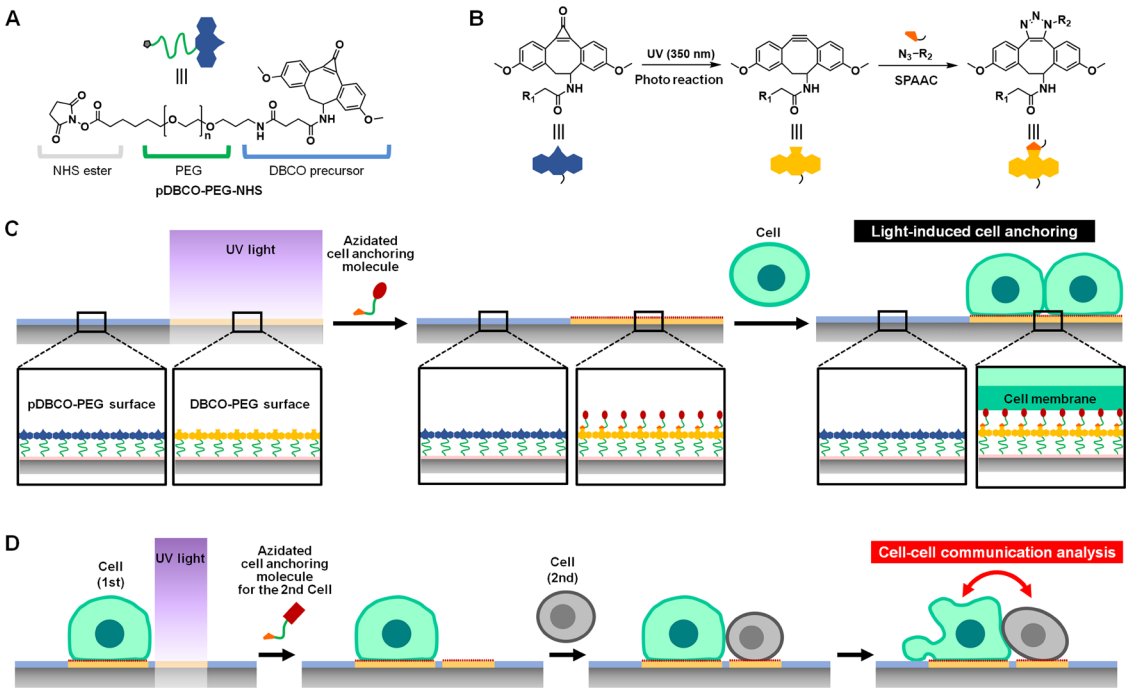

Figure 1. Photoreactive substrate-coating material and light-induced cell anchoring. (A) Chemical structure of a photoreactive substrate-coating material, pDBCO-PEG-NHS, comprising a photoreactive dibenzocyclooctyne (DBCO) precursor, bioinert poly(ethylene glycol) (PEG), and NHS ester for surface modification. (B) Schematic of the photoreaction of the DBCO precursor and "click" reaction (strain-promoted alkyne-azide cycloadditions: SPAAC) with an azide group. (C) Schematic of the light-induced cell patterning procedure. The desired region of the pDBCO-PEG-NHS-coated surface is exposed to UV light. Azidated cell anchoring molecules are then added to the light-exposed surface via the SPAAC reaction with the photoconverted DBCO moiety. Cells are selectively anchored on the desired region by binding to the cell anchoring molecules. (D) Schematic of the intercellular communication analysis between the heterogeneous cell pairs positioned by light-induced anchoring.

during attachment of the second cell. Therefore, a photoactivatable surface that can rapidly anchor any kind of cell is required for ideal cell pairing and to analyze a wide variety of intercellular communications. Recently, we reported a photoactivatable material for rapidly anchoring any type of cell through the interaction between the lipid moiety of the material and cell membrane.[18] However, the cell anchoring function of the material is blocked when incubated with serum, and therefore, all cells must be anchored before incubation. The preparation of single-cell pairs with conventional photoactivatable materials is currently restricted in principle.

In this study, we report the first use of a photoreactive material for precise and rapid attachment of any type of cell to a substrate surface via light-induced conjugation with cell anchoring molecules. Since in principle any cell anchoring molecules can be conjugated at the desired timing, both adherent and non-adherent cells are attached onto the surface on any desired time schedule. By employing the cell anchoring molecules that can rapidly and selectively bind to cell surfaces, rapid and selective cell attachment may be achieved, respectively. Thus, compared with the conventional surfaces of photoactivating a single cell-anchoring molecule, the present approach is considered to have the advantage that the cell attachment is flexibly designed by utilizing appropriate cell anchoring molecules according to the application. As illustrated in Figure 1, a photoreactive material was designed to selectively and bioorthogonally conjugate with a variety of cell anchoring molecules in only light-exposed regions. We used the photoactivatable precursor of dibenzocyclooctyne (DBCO), abbreviated pDBCO,[19] as the photoreactive moiety. The pDBCO moiety is attached to the end of a long hydrophilic and flexible PEG chain (Mn: 5000 (g/mol)), and the other end of the PEG has an activated ester group for modification of the substrate surface (Figure 1A). The pDBCO moieties are supported at the surface of the PEG layer, which is widely used for inhibiting the non-specific adhesion of living cells.[20] By exposure to ultraviolet (UV) light, this pDBCO moiety is converted to DBCO, which reacts to an azide group under a physiological condition via copper-free Huisgen cycloaddition (Figure 1B). Therefore, cell anchoring molecules with azide groups can be immobilized selectively at light-exposed surfaces, and the cells are selectively anchored on the light-exposed region by binding to cell anchoring molecules without non-specific adhesion to non-light-exposed surfaces (Figure 1C). Multiple types of cells can be simply and precisely positioned on the flat substrate by repeating these procedures. The sequential exposure of the adjacent regions to light enables cell pairing for monitoring intercellular communication between the heterogeneous cells at the single-cell level (Figure 1D). We demonstrate light-induced cell anchoring using three azidated cell anchoring molecules and show that the surface is a valuable tool for image-based analysis of intercellular communications in immunology.

RESULTS

Synthesis and Characterization of Photoreactive Materials. The photoreactive coating material, pDBCO-PEG-NHS, was synthesized in five steps (Figure S1A). To evaluate the photoconversion of pDBCO at the end of PEG, the UV–visible absorbance spectra of the solution of compound **5** (pDBCO-PEG-COOH) were measured after exposure to various amounts of 365 nm light (Figure S1B,C). The photoconversion was finished below 1.0 J/cm^2 in a high-

https://doi.org/10.1021/jacs.2c07321
J. Am. Chem. Soc. XXXX, XXX, XXX−XXX

concentration solution (conc.: 100 μM, volume: 200 μL) considering the disappearance of the specific absorbance of pDBCO at 353 nm. After light exposure (greater than 8 J/cm^2), perfect conversion to DBCO was confirmed using ^{1}H-NMR spectroscopy (Figure S2). The pDBCO-PEG conjugate was successfully converted to the DBCO-PEG conjugate by light under aqueous conditions. In addition, the pDBCO moiety was confirmed to be stable in aqueous solution for more than 24 h, even with nucleophilic moieties that are in cell culture conditions such as amine and thiol (Figure S3).

The light-induced reaction of the material-modified surface was then evaluated. A collagen-coated cover glass was modified with pDBCO-PEG-NHS via an amide coupling reaction. The modified glass surface was exposed to light and then treated with an azide-modified red fluorescent dye (Alexa Fluor 594-azide) to examine the reaction with azide-modified molecules after photoconversion. After washing to remove free dye, the fluorescence of the surface was observed with a confocal microscope followed by image analysis for quantification. On the surfaces exposed to light exceeding 0.1 J/cm^2, the red fluorescence was clearly greater than the unexposed surface (Figure S4). The fluorescence was comparable to the positive control surface on which the photoconverted material, DBCO-PEG-NHS, was modified. As a result, nearly all pDBCO moieties on the surface were converted to DBCO by light exposure at 0.1 J/cm^2 (more than 2 mW/cm^2 within 50 s) and reacted with azide-modified dye. Therefore, we used this light exposure condition in subsequent experiments.

Light-Induced Cell Anchoring. Light-induced cell anchoring was performed on the photoreactive surface by employing PEG-lipid as a cell anchoring molecule. Materials comprising hydrophilic polymers and lipids are used for interacting with the lipid bilayer membranes of cell surfaces,[21] and particularly, PEG-lipids can anchor any type of cells on their coated surfaces without cytotoxicity.[22−25] It is worth noting that cells can be rapidly and tightly anchored within 5 min. Such features are suitable for demonstrating spatio-temporal anchoring of multiple kinds of cells on a substrate. A PEG-oleoyl was conjugated to an azide group (Supporting Information), and this azidated PEG-lipid (Lipid-PEG-azide) was used for light-induced cell anchoring (Figure 2A,B). In this study, we adopted a microchannel system to examine selective cell anchoring to the substrate (Figure S5). In this system, the cells on the whole surface of the microchannel can be uniformly rinsed using laminar flow. Therefore, the cells that are weakly anchored via non-specific interactions and specific interactions with insufficient strength against the flow are washed out. After exposure to a line pattern of light, the photoreactive surface was treated with Lipid-PEG-azide in the microchannel. The murine pro-B BaF3 cell that expresses enhanced green fluorescent protein (EGFP) as a fluorescent label (EGFP-BaF3) was applied to the surface (Figure 2B). After rinsing the surface, a line pattern of cells was clearly observed with high contrast, and the cells were anchored only on the light-exposed region as expected (Figure 2C,D). It is worth noting that nearly all cells were washed out in the unexposed regions, which indicates that the surface can anchor non-adherent cells selectively in the light-exposed region by strictly inhibiting non-specific adsorption. Similar light-induced cell patterning was successfully demonstrated after incubation for 1 day in a cell culture condition with serum (Figure S6).

Next, multi-colored cells were anchored stepwise at each defined region in a light-induced manner. In this experiment, EGFP-BaF3 cells (green) were used, and human T cell leukemia

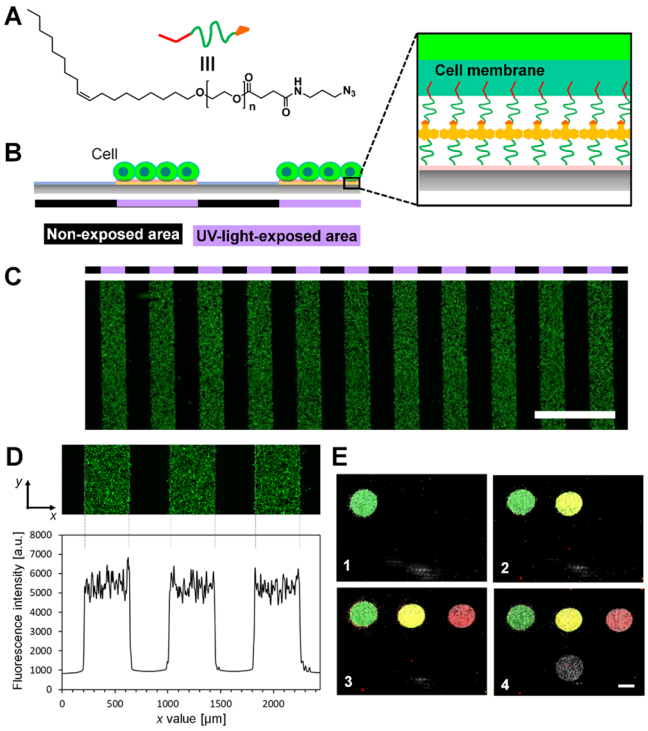

Figure 2. Light-induced cell anchoring. (A) Chemical structure of an azidated PEG-lipid, Lipid-PEG-azide. (B) Schematic illustration of light-induced cell anchoring with Lipid-PEG-azide. (C) Fluorescence microscopic image of anchored enhanced green fluorescent protein (EGFP)-expressing BaF3 cells (EGFP-BaF3) in a line pattern. Scale bar: 1000 μm. (D) Fluorescence intensity of the EGFP-BaF3 cell-anchored surface. The mean intensity of the *y* position was determined at each *x* position (bottom) in the enlarged fluorescence image of panel (C) (top). (E) Fluorescence microscopic images of the multi-colored cells in the allocated spots. (1) EGFP-BaF3 cell (green), (2) green and red fluorescent dye-stained Jurkat cells (yellow), (3) red fluorescent dye-stained Jurkat cells (red), and (4) non-stained Jurkat cells were positioned in a light-induced manner in numerical order. The merged green and red fluorescent images at each step are represented. Scale bar: 500 μm.

Jurkat cells were used after staining with only a red fluorophore (red) and doubly with a green and red fluorophore (yellow). After anchoring the EGFP-BaF3 cells, the other region was exposed to the light followed by treatment with Lipid-PEG-azide. The stained yellow cells were applied to the surface. After rinsing, the spot of yellow cells was observed without cross-contamination with the first green cell spot (Figure 2E, upper right). Similarly, red stained and unstained cells could be successively positioned at the defined light-exposed regions by repeating the procedures described above (Figure 2E, bottom left and right). Thus, fine patterns of multiple cells were rapidly constructed on the surface.

Cell Anchoring with Lectins and Antibodies. To demonstrate the versatility of the photoreactive surface, we employed other cell anchoring molecules. First, glycan-binding protein, lectin, was used. Here, rBC2LCN is the recombinant *N*-terminal domain of lectin (BC2L-C) isolated from *Burkholderia cenocepacia* that binds to the fucose moieties on cell surface glycans and binds exclusively to undifferentiated human induced pluripotent stem (iPS) cells.[26] Azide-modified rBC2LCN (rBC2LCN-azide) was prepared by an azidation reagent and then applied to the photoreactive surface to expose a line pattern (Figure 3A). A mixture of green fluorescent-stained iPS cells and

https://doi.org/10.1021/jacs.2c07321
J. Am. Chem. Soc. XXXX, XXX, XXX−XXX

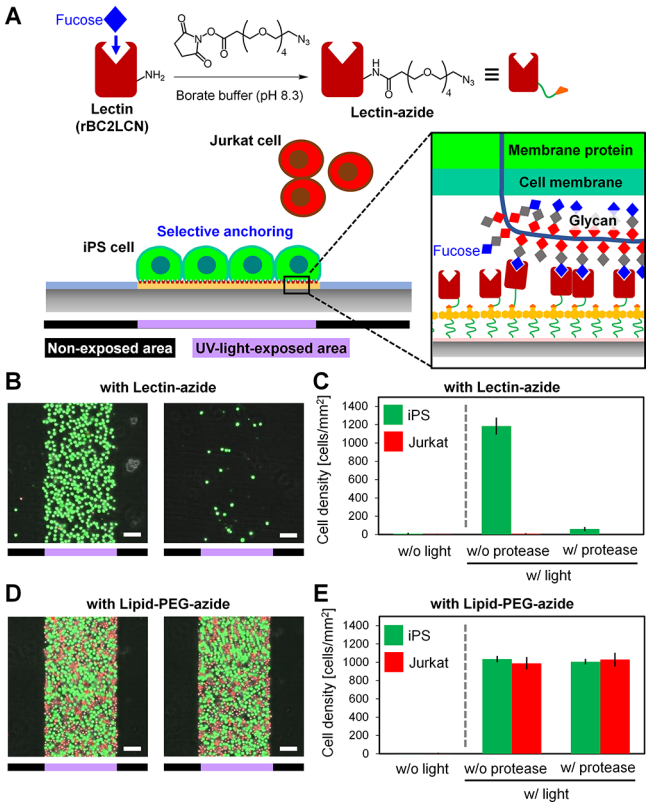

Figure 3. Light-induced anchoring and enzymatic release of an iPS cell. (A) Schematic illustration of iPS cell anchoring using azidated lectin (lectin-azide). rBC2LCN lectin was used because it specifically binds to undifferentiated iPS cells. (B) Fluorescence microscopic images of the cells anchored with lectin-azide in a line pattern before (left) and after protease treatment (right). The mixture of green fluorescent dye-stained iPS cells and red fluorescent dye-stained Jurkat cells was applied to the light-exposed surfaces. Scale bars: 100 μm. (C) Densities of the cells anchored with lectin-azide at the unexposed and light-exposed regions before and after protease treatment in the images shown in panel (B). Values and error bars represent mean ± standard errors (n = 10). (D) Fluorescence microscopic images of the cells anchored with azidated PEG-lipid (Lipid-PEG-azide) observed in the same way as panel (B). Scale bars: 100 μm. (E) Densities of the cells anchored with Lipid-PEG-azide in the images shown in panel (D). Values and error bars represent mean ± standard errors (n = 10).

red fluorescent-stained Jurkat cells was applied to the lectin-treated surface. After rinsing the surface, iPS cells were selectively anchored to the light-exposed regions (Figure 3B,C). Furthermore, after a treatment with protease for 10 min, most of the anchored iPS cells were detached from the surface (Figure 3B,C). This cell mixture was also applied to the photoreactive surface treated with Lipid-PEG-azide. On the PEG-lipid surface, both iPS cells and Jurkat cells were anchored and not detached by the protease treatment (Figure 3D,E). These results clearly indicate that the iPS cells were anchored to the lectin-conjugated surface via the specific interaction of lectin to the fucose moiety on cell surfaces. Thus, by using cell anchoring molecules with cell selectivity, only the target cell in the cell mixture could be anchored at the desired position that was light defined.

Next, we used an antibody as another useful cell anchoring molecule. In a preliminary experiment in which an azide-modified antibody reacted with the surface, non-specific cell adhesion was observed in the unexposed regions (Figure S7). This non-specific adsorption became more pronounced as the treatment time with the antibody exceeded 15 min. In this approach, a certain time was required for the reaction between azide and DBCO on the surface. Therefore, another approach that reduces the antibody treatment time was necessary. Here, we used an antibody-binding protein, protein G, as the anchor for the antibody. In this approach, azide-modified protein G (G-azide) was prepared and applied to the light-exposed photoreactive surfaces (Figure 4A). Antibodies can quickly attach to a

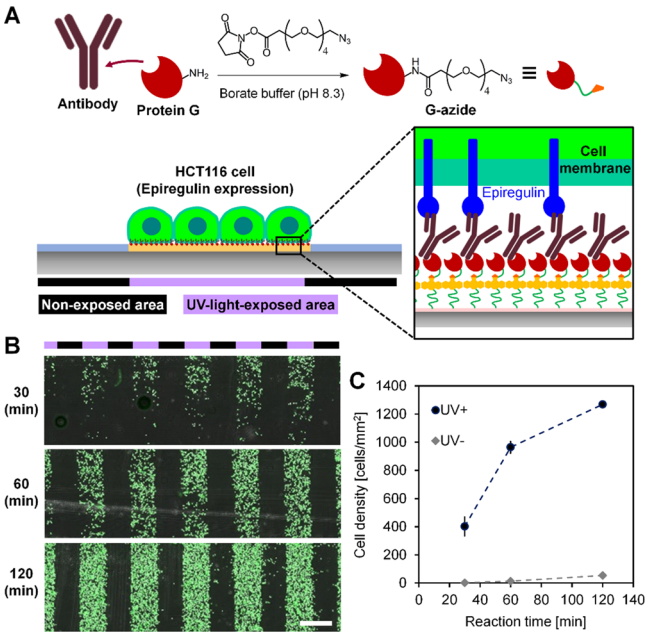

Figure 4. Light-induced cell anchoring with an antibody. (A) Schematic illustration of the anchoring of antigen-expressing cells using an azidated protein G (G-azide) and antibody. An epiregulin-expressing HCT116 cell was anchored with the anti-epiregulin antibody (9E5) via light-induced modification of G-azide. (B) Fluorescence microscopic images of the anchored cells on the surface treated with G-azide for various periods (30, 60, and 120 min). The HCT116 cells were fluorescently stained green. Scale bar: 500 μm. (C) Cell density as function of the G-azide treatment period at the non-light-exposed and light-exposed regions in the images shown in panel (B). Values and error bars represent mean ± standard errors (n = 10).

protein G-conjugated surface. For example, an anti-epiregulin antibody (9E5)[27] was applied to the G-azide-treated surface for 10 min, and then, human colon cancer HCT116 cells, which highly express epiregulin on the plasma membrane,[27,28] were applied (Figure 4A). The green fluorescent-stained HCT116 cells were successfully anchored in a line pattern (Figure 4B). As the treatment time of G-azide increased, the density of anchored cells increased in the light-exposed regions, whereas the non-specific cell anchoring was negligible (Figure 4C). Thus, by using G-azide in the present system, an intact antibody could be rapidly attached to the photoreactive surface, and antigen-expressing cells were anchored in a light-guided manner without significant non-specific adhesion. Furthermore, in this protein G-mediated method, a variety of antibodies can be used without azidation, and this simplicity is advantageous for anchoring cells selectively using the specificity of the antibody.

Fabrication of a Single-Cell Array and Single-Cell Pairs. To construct the microarray of cell pairs, single cells were positioned on the photoreactive surface in a light-induced manner. A light-exposure system based on a digital mirror device

https://doi.org/10.1021/jacs.2c07321
J. Am. Chem. Soc. XXXX, XXX, XXX−XXX

was used for the miniaturization of the light spots to a single-cell size. In this experiment, a Jurkat cell was used as the model cell, and Lipid-PEG-azide was used as the cell anchoring molecule. The photoreactive surfaces were exposed to round spots of light with various diameters from 10 to 30 μm in a grid. By successive treatment with Lipid-PEG-azide and Jurkat cells, cell microarrays were created on the surfaces (Figure 5A). According to

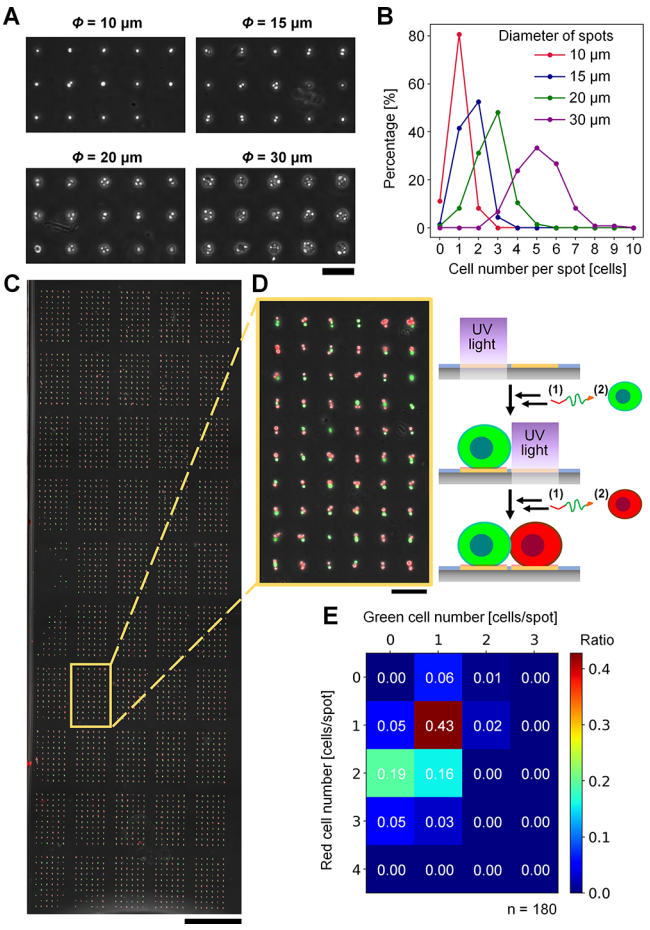

Figure 5. Light-induced cell anchoring at the single-cell level. (A) Phase-contrast microscopic images of the array of Jurkat cells on the surface exposed to various diameters of light spots. Scale bar: 100 μm. (B) Percentage of spots containing various numbers of anchored cells. The cell number at each spot was counted at 135 spots with various diameters of 10, 15, 20, and 30 μm. (C) Fluorescence microscopic image of an array of two different colored heterogeneous single-cell pairs. The green and red fluorescently stained Jurkat cells were anchored at each allocated spot. The merged green and red fluorescent images are represented. Scale bar: 1000 μm. (D) Enlarged image of single-cell pairs in the image of panel (C). Scale bar: 100 μm. (E) Matrix of the ratio of each spot containing various numbers of green and red fluorescent cells. The cell number was counted at 180 spots.

the diameter of the light spots, the number of anchored cells at each spot varied. At a diameter of 10 μm, 80% of the spots were occupied by a single cell, whereas 12 and 8% were occupied by zero and two cells, respectively (Figure 5B). At larger diameters, more than two cells were typically arrayed, and the rate of single cells drastically decreased as the diameter increased. From these results, the 10 μm diameter was optimal for positioning single Jurkat cells.

By repeating the procedure for single-cell positioning, colored Jurkat cells (green and red) were arrayed stepwise to prepare an array of pairs. An array of several thousands of cell pairs was constructed on the surface (Figure 5C). In this system, cell pairs were observed within 15 min after loading red-stained cells as the second cell because of rapid cell anchoring. In the expanded images, the single-cell pairs of green- and red-stained cells were confirmed as expected (Figure 5D). From image analysis, the single-cell pair of two different colored cells was 43% (Figure 5E). Thus, a large number of single-cell pairs, mainly heterogeneous cells, were successfully constructed on a flat substrate surface without microstructures or microwells.

Single-Cell Observation of Intercellular Communications. Finally, we demonstrated that the photoreactive surface can be applied to single-cell observation of the intercellular interactions between human primary natural killer (NK) cells and human chronic myeloid leukemia K562 cells. NK cells are lymphocytes that contribute to the early immune response to pathogens,[29] and the functional exhaustion of NK cells is correlated with the progression of diseases such as malignant tumors[30] and viral infections including COVID-19.[31,32] Therefore, the cytotoxicity of NK cells has recently attracted attention as a target for diagnosis and therapy.[30−32] K562 cells have been widely used as a standard target in the analysis of human NK cell cytotoxicity.[33] In this experiment, single-cell pairs of a NK cell and K562 cell were produced to observe the cytotoxicity of the NK cell. The K562 cell was stained with calcein-AM to evaluate the perturbation of the cell membrane by the lytic attack of the NK cell. In some time-lapse images of the anchored single-cell pairs, the K562 cell was observed to contact the neighboring NK cell, and then the cell started to shrink with dynamically forming small blebs, finally followed by fragmentation (Figure 6A and Movie S1). In such cases, the green fluorescence of the K562 cell started to decrease with the blebbing and then disappeared by fragmentation (Figure 6B). These morphological features are typically observed in apoptotic cell death.[34] In other images, the K562 cell rapidly swelled with a large bleb and the fluorescence disappeared (Figure 6C,D and Movie S2). Such features are observed in necrotic cell death.[34] The time course of the cytotoxic events on each K562 cell was identified by observing the time-lapse images of 18 NK-K562 cell pairs in detail (Figure 6E). In this study, 57 and 21% of the K562 cells were induced to apoptosis-like and necrosis-like death, respectively. It is reported that the NK cell induces K562 cell death by apoptosis and necrosis via contact.[34] Therefore, the results on the photoreactive material surface are consistent with previous studies that used ordinary culture dishes and painstakingly identified heterogeneous NK-K562 cell pairs that happened to interact with each other in a mixed cell population.

In the time-lapse images, the fluorescence of the K562 cell decreased via contact with the NK cell because of perturbation of the membrane and dye leaking. NK cells induce membrane perturbation by releasing cytotoxic granules containing perforin and granzyme B;[35] this event is called lytic hit. In the time course of fluorescence, the first significant decrease was derived from the lytic hit (Figure 6B,D). The fluorescence change of each K562 cell at the lytic hit was plotted versus the time period between their first contact and lytic hit (Figure 6F). In this plot, the single-cell pairs were divided into two main categories: a large decrease in the fluorescence within a shorter period and a small fluorescence decrease induced after various times. Most of the cell pairs with necrosis-like death were categorized as a large and rapidly decreasing fluorescence, and those with apoptosis-like death were in the other category (Figure 6F). Here, the observed cytotoxicity is assumed to be mainly the perforin/

https://doi.org/10.1021/jacs.2c07321
J. Am. Chem. Soc. XXXX, XXX, XXX−XXX

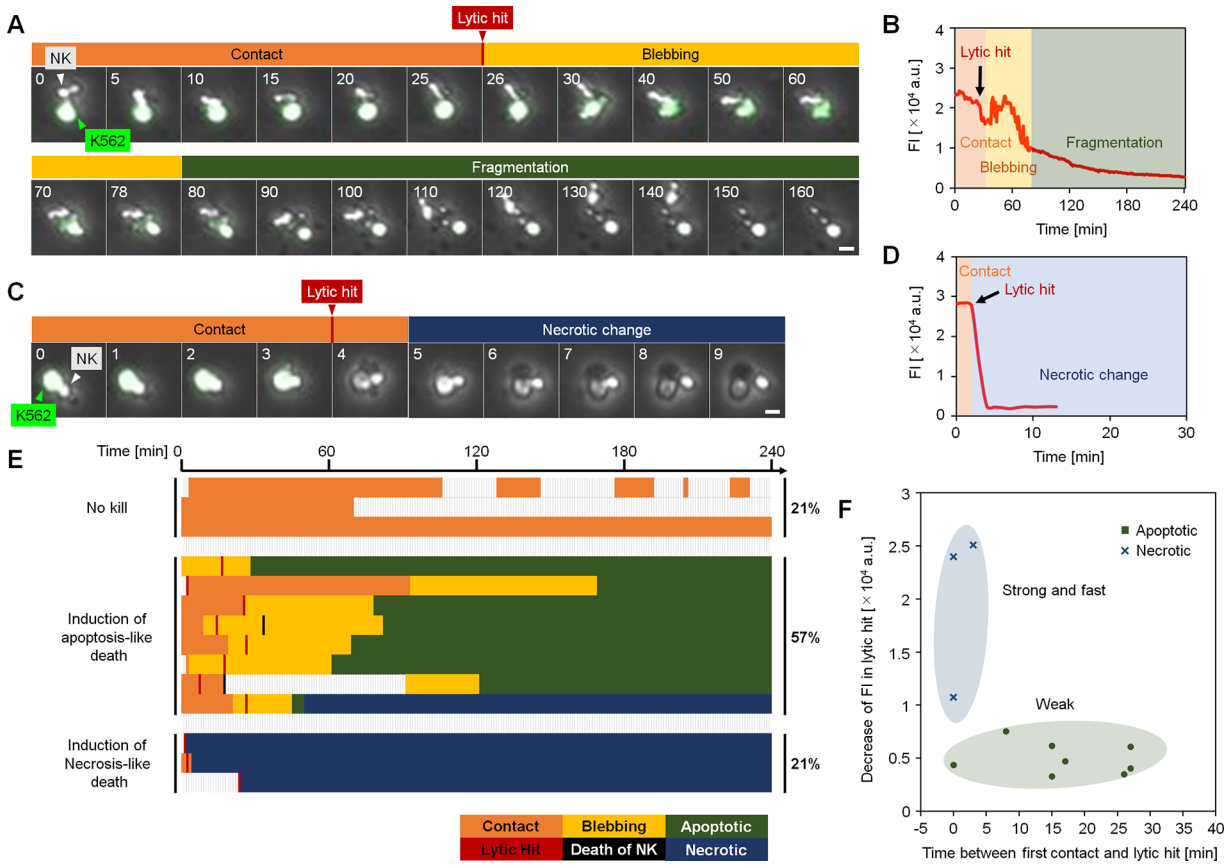

Figure 6. Single-cell analysis of the cytotoxic interaction of an immunocyte and leukemic cell. (A, C) Time-lapse images of a single-cell pair of a natural killer (NK) cell and leukemic cell, K562 cell. The K562 cell was stained with a live cell stain, calcein-AM. The number in each image represents the observation time (min). Scale bar: 10 μm. (B, D) Time course of the fluorescence intensity of the K562 cell in the image of panels (A, C). The first drastic decrease in fluorescence intensity (FI) was defined as the lytic hit from the NK cell. The periods of blebbing and fragmentation were determined from the morphology of K562 cells in panels (A, C). (E) Chart of the processes in the cytotoxic interaction of each cell pair. The death of the K562 cell was identified by the disappearance of fluorescence, and the apoptosis- and necrosis-like death were distinguished from the cellular morphology in individual time-lapse images. (F) Plots of the decrease in FI in the lytic hit versus the time length between the starting time of the intercellular contact and time of the lytic hit. The plots were largely separated into the two groups that correlate with the apoptosis- and necrosis-like death in the chart of panel (E).

granzyme pathway because K562 cells express no FasR.[36] Moreover, in the K562 cell killing of the NK cell, the apoptosis and necrosis were reported to be induced at low and high concentrations of cytotoxic granules, respectively.[34] Therefore, the present necrosis-like death with drastic and rapid perturbation of the cell membrane may be reflected by the secretion of large amounts of cytotoxic granules at the contact faces of the cell pairs. Thus, the single-cell pairs in the image are assumed to reflect the activity of individual cytotoxic lymphocytes in their communication.

DISCUSSION

We developed a photoreactive material for precise light-induced anchoring of living cells on a substrate surface. In comparison to conventional photoactivatable cell anchoring surfaces, our photoreactive surface offers several advantages. The photoreactive pDBCO moiety we used adopts light-induced conjugation with various azidated molecules for cell anchoring via a bioorthogonal and biocompatible "click" reaction.[19] Various cell anchoring molecules, such as PEG-lipid, lectin, and antibodies, were selectively attached at the light-exposed regions for cell anchoring. By selecting proper cell anchoring molecules, the surface realized light-induced anchoring of a variety of cells such as leukemia cells, iPS cells, epithelial carcinoma cells, and primary immune cells, regardless of the cell adhesiveness typically required for conventional surfaces applicable to only adherent cells.[14−17] In particular, by using an azidated PEG-lipid, the light-exposed regions were rapidly and completely filled with anchored cells after only a 10 min incubation. The cell anchoring in this study is faster than other cell adhesion-based approaches.[14−17] By using selective cell anchoring molecules, the cell of interest in cell mixtures can be selectively anchored and potentially used for single-cell analysis. This function is original and promising for the analysis of biological and medical samples, including a number of cell types. In its molecular design, the material consists of a conjugate of the photoreactive moiety with a long PEG chain to block non-specific cell adsorption. The present material-modified surface realized light-induced cell anchoring without non-specific cell adsorption, achieving cell patterns with high contrast. Advantages in versatility, rapidity, and selectivity will contribute to the high efficiency pairing of heterogeneous cells of interest without preparative cell sorting.

We applied our platform surface for single-cell pairing to observe the cytotoxicity of immune cells at the single-cell level. K562 cells were rapidly anchored near NK cells for cell pairing, leading to precise timing of the contact initiation, and only a

https://doi.org/10.1021/jacs.2c07321
J. Am. Chem. Soc. XXXX, XXX, XXX−XXX

small portion of cell pairs started their contact before observation (Figure 6E). On the present array of K562-NK cell pairs, dynamic and large morphological changes, such as the formation of a large bleb, were clearly observed, similar to those on ordinary culture dishes.[34] In the conventional MEMS-based methods, where cell pairs are constructed by successively pushing cells into the narrow space of the microstructures such as microwells, it is difficult to observe morphological changes without bias because the cells are surrounded by solid walls.[6−8] On this study's flat surface without a microstructure, the two types of cell deaths, apoptosis-like and necrosis-like, were distinguished by dynamic morphologies. Although further studies elucidating the molecular mechanisms of the two types of cell deaths are needed, the present method is a promising platform for analyzing the activity and exhaustion of immune cells at a single-cell level. Compared with conventional cytotoxicity assays based on the average of a large cell population, this single-cell analysis may contribute to quantifying specific cell populations with unique cytotoxicity in blood and other specimens. Furthermore, by using the dynamic and flexible anchoring of this photoreactive system, the number, distance, timing, and relative position of the component cells in intercellular communications are freely designed and dynamically changed. Such a unique analysis system may provide new insight into immunological systems by identifying the unknown parameters critical for cytotoxicity.

CONCLUSIONS

The presented photoreactive material provides a versatile substrate surface for light-induced anchoring of living cells. The photoreactive moiety is stable, and therefore, the light-induced cell anchoring function is retained under culture conditions. On the surface of this material, the cell anchoring molecule can be selected, depending on the cell type and the purpose of the experiment. Because of the biocompatibility and bioorthogonality of the light-induced cell anchoring process, multiple cells can be positioned on the same surface. On the basis of these achievements and advantages, the surface provides a promising method for single-cell pairing to evaluate intercellular communication with a variety of cell types and morphological changes on the flat substrate surface. In principle, we expect to enable comprehensive image-based analysis of intercellular communications and contribute to the identification of a new target morphological feature for drug discovery and diagnosis of incurable diseases. Single-cell sorting based on intercellular communication images can be achieved with this platform surface, potentially leading to identification of the disease-related marker genes and rapid screening of therapeutic cytotoxic immune cells in the near future.

EXPERIMENTAL SECTION

Synthesis of a Photoreactive Material and Azidated Reagents. Synthetic protocols are detailed in the Supporting Information. Briefly, pDBCO-PEG-NHS was synthesized by adding the photoreactive DBCO precursor to the end of a PEG chain. The photoreactive DBCO precursor was synthesized based on a previous report[37] with modifications. The DBCO precursor was conjugated with amino-PEG-carboxylic acid (Mw: 3400, Sunbright PA-034HC, NOF Co., Tokyo, Japan) by a reaction between the NHS ester and amine group. The carboxyl group at the other end of the PEG chain was converted to NHS ester for modification of the surface.

Lipid-PEG-NHS (Mw: 4000, Sunbright OE-040CS, NOF Co.) was conjugated with azide propylamine to obtain Lipid-PEG-azide. An antibody, protein G, and lectin were conjugated with NHS-PEG_4-azide to obtain azidated proteins.

Modification of the Substrate Surfaces. Modification protocols are detailed in the Supporting Information. Briefly, glass slides and coverslips were coated by immersing the substrates in type I collagen solution (Cellmatrix, Nitta Gelatin, Osaka, Japan). After washing the coated surface with MilliQ water (Millipore Inc., Bedford, MA, USA), a solution of pDBCO-PEG-NHS in ethanol (20 μM) was applied to the surface and dried.

Light-Induced Cell Attachment and Single-Cell Array. A microchannel (width: 3.8 mm, length: 18 mm, height: 0.40 mm, Ibidi GmbH, Munich, Germany) was mounted on the surface modified with pDBCO-PEG-NHS. The substrate surface was exposed to 365 nm wavelength light with an ultraviolet (UV) irradiator equipped with a cylindrical lens (MAX-302, Asahi Spectra Co., Ltd., Tokyo, Japan) through a photomask with a line pattern. A solution of the azidated reagent (Lipid-PEG-azide: 50 or 100 μM, azidated antibody: 1 μM, azidated protein G: 20 μM, azidated lectin: 25 μM) in PBS was injected into the microchannel and incubated for 2 h at room temperature. After rinsing the substrate surface with PBS, a cell suspension (1×10^7 cells/mL) in PBS was loaded into the microchannel and incubated for 10 min at room temperature. After removing the cell suspension, the substrate surface was washed with PBS, and the phase contrast and fluorescence images of the surface were obtained with a fluorescence microscope (IX83, Olympus Co., Tokyo, Japan). The fluorescence intensity and number of anchored cells were analyzed with ImageJ (NIH, Bethesda, MD, USA). In the micropatterning of multi-colored cells, the surface was exposed to a spot of light from the xenon lamp of the fluorescence microscope via the band-pass filter (350/390) followed by modification with Lipid-PEG-azide and anchoring of a stained cell. Other regions of the surface were exposed to light, modification, and anchoring of the other stained cell; this procedure was repeated at different regions using each stained cell. In the preparation of a single-cell array, the substrate surface was exposed to a fine pattern of light spots (365 nm, 0.8 or 1.6 J/cm^2) with a maskless lithography system (PALET, NEOARK Co., Tokyo, Japan) followed by modification with Lipid-PEG-azide and cell anchoring as described above. The number of anchored cells at each light-exposed spot was counted from nine randomly selected regions containing 3 × 5 spots (total 135 spots).

Fabrication of Single-Cell Pairs. The substrate surface of each microchannel was exposed to 3000 spots of light with diameters of 10 μm followed by Lipid-PEG-azide modification. After anchoring of the first cell, the neighboring region to each anchored cell was exposed to the spot of light in the same way. In the region, Lipid-PEG-azide was modified, and then, the second cell was anchored to construct the neighboring cell pair. The array of cell pairs was observed with the fluorescence microscope, and the number of heterogeneous cell pairs was counted using ImageJ.

Cytotoxicity of NK Cells against K562 Cells. An array of single-cell pairs of NK cells and K562 cells was prepared as described above. The array was incubated in the NK cell culture medium at 37 °C in a humidified atmosphere containing 5% CO_2. Time-lapse images were obtained every minute for 4 h and analyzed by ImageJ.

ASSOCIATED CONTENT

Supporting Information

The Supporting Information is available free of charge at https://pubs.acs.org/doi/10.1021/jacs.2c07321.

Apoptosis-like death of the K562 cell observed in a single-cell pair with the human NK cell (AVI)

Necrosis-like death of the K562 cell observed in a single-cell pair with the human NK cell (AVI)

Additional experimental details, materials, and methods including photographs of the experimental setup, ^{1}H NMR spectra for all compounds, and ^{13}C NMR spectra and mass spectra for novel compounds (PDF)

https://doi.org/10.1021/jacs.2c07321
J. Am. Chem. Soc. XXXX, XXX, XXX−XXX

AUTHOR INFORMATION

Corresponding Authors

Satoshi Yamaguchi − *Department of Chemistry & Biotechnology, Graduate School of Engineering, The University of Tokyo, Tokyo 113-8656, Japan; PRESTO, Japan Science and Technology Agency (JST), Tokyo 102-0076, Japan;* orcid.org/0000-0003-4822-7469; Phone: +81-3-5452-5202; Email: yamaguchi@chembio.t.u-tokyo.ac.jp; Fax: +81-3-5452-5209

Akimitsu Okamoto − *Department of Chemistry & Biotechnology, Graduate School of Engineering, The University of Tokyo, Tokyo 113-8656, Japan;* orcid.org/0000-0002-7418-6237; Phone: +81-3-5452-5201; Email: okamoto@chembio.t.u-tokyo.ac.jp; Fax: +81-3-5452-5209

Authors

Takahiro Kosaka − *Department of Chemistry & Biotechnology, Graduate School of Engineering, The University of Tokyo, Tokyo 113-8656, Japan*

Shin Izuta − *Department of Chemistry & Biotechnology, Graduate School of Engineering, The University of Tokyo, Tokyo 113-8656, Japan*

Shinya Yamahira − *Center for Medical Sciences, St. Luke's International University, Tokyo 104-8560, Japan*

Yoshikazu Shibasaki − *Research Center for Advanced Science and Technology (RCAST), The University of Tokyo, Tokyo 153-8904, Japan*

Hiroaki Tateno − *Cellular and Molecular Biotechnology Research Institute, National Institute of Advanced Industrial Science and Technology (AIST), Tsukuba, Ibaraki 305-8566, Japan*

Complete contact information is available at: https://pubs.acs.org/10.1021/jacs.2c07321

Notes

The authors declare no competing financial interest.

ACKNOWLEDGMENTS

This research was supported by the Japan Science and Technology Agency (JST) PRESTO 16815021, the MIRAI program 19217334, and a Grant-in-Aid from the Japan Society for the Promotion of Science (JSPS) Research Fellows 20J22920. We thank Ashleigh Cooper, PhD, from Edanz (https://jp.edanz.com/ac) for editing a draft of this manuscript.

REFERENCES

(1) Lawson, D. A.; Kessenbrock, K.; Davis, R. T.; Pervolarakis, N.; Werb, Z. Tumour Heterogeneity and Metastasis at Single-Cell Resolution. *Nat. Cell Biol.* **2018**, *20*, 1349−1360.

(2) Papalexi, E.; Satija, R. Single-Cell RNA Sequencing to Explore Immune Cell Heterogeneity. *Nat. Rev. Immunol.* **2018**, *18*, 35−45.

(3) Keller, L.; Pantel, K. Unravelling Tumour Heterogeneity by Single-Cell Profiling of Circulating Tumour Cells. *Nat. Rev. Cancer* **2019**, *19*, 553−567.

(4) Eichmann, A.; Corbel, C.; Nataf, V.; Vaigot, P.; Bréant, C.; Le Douarin, N. M. Ligand-Dependent Development of the Endothelial and Hemopoietic Lineages from Embryonic Mesodermal Cells Expressing Vascular Endothelial Growth Factor Receptor 2. *Proc. Natl. Acad. Sci.* **1997**, *94*, 5141−5146.

(5) Ramilowski, J. A.; Goldberg, T.; Harshbarger, J.; Kloppmann, E.; Lizio, M.; Satagopam, V. P.; Itoh, M.; Kawaji, H.; Carninci, P.; Rost, B.; Forrest, A. R. R. A Draft Network of Ligand−Receptor-Mediated Multicellular Signalling in Human. *Nat. Commun.* **2015**, *6*, 7866.

(6) Dura, B.; Dougan, S. K.; Barisa, M.; Hoehl, M. M.; Lo, C. T.; Ploegh, H. L.; Voldman, J. Profiling Lymphocyte Interactions at the Single-Cell Level by Microfluidic Cell Pairing. *Nat. Commun.* **2015**, *6*, 5940.

(7) Dura, B.; Servos, M. M.; Barry, R. M.; Ploegh, H. L.; Dougan, S. K.; Voldman, J. Longitudinal Multiparameter Assay of Lymphocyte Interactions from Onset by Microfluidic Cell Pairing and Culture. *Proc. Natl. Acad. Sci.* **2016**, *113*, E3599−E3608.

(8) Jang, J. H.; Huang, Y.; Zheng, P.; Jo, M. C.; Bertolet, G.; Zhu, M. X.; Qin, L.; Liu, D. Imaging of Cell−Cell Communication in a Vertical Orientation Reveals High-Resolution Structure of Immunological Synapse and Novel PD-1 Dynamics. *J. Immunol.* **2015**, *195*, 1320−1330.

(9) Yoshimura, Y.; Tomita, M.; Mizutani, F.; Yasukawa, T. Cell Pairing Using Microwell Array Electrodes Based on Dielectrophoresis. *Anal. Chem.* **2014**, *86*, 6818−6822.

(10) Vu, T. Q.; de Castro, R. M. B.; Qin, L. Bridging the Gap: Microfluidic Devices for Short and Long Distance Cell−Cell Communication. *Lab Chip* **2017**, *17*, 1009−1023.

(11) Sarkar, S.; Sabhachandani, P.; Stroopinsky, D.; Palmer, K.; Cohen, N.; Rosenblatt, J.; Avigan, D.; Konry, T. Dynamic Analysis of Immune and Cancer Cell Interactions at Single Cell Level in Microfluidic Droplets. *Biomicrofluidics* **2016**, *10*, No. 054115.

(12) Sarkar, S.; Sabhachandani, P.; Ravi, D.; Potdar, S.; Purvey, S.; Beheshti, A.; Evens, A. M.; Konry, T. Dynamic Analysis of Human Natural Killer Cell Response at Single-Cell Resolution in B-Cell Non-Hodgkin Lymphoma. *Front. Immunol.* **2017**, *8*, 1−13.

(13) Madrigal, J. L.; Schoepp, N. G.; Xu, L.; Powell, C. S.; Delley, C. L.; Siltanen, C. A.; Danao, J.; Srinivasan, M.; Cole, R. H.; Abate, A. R. Characterizing Cell Interactions at Scale with Made-to-Order Droplet Ensembles (MODEs). *Proc. Natl. Acad. Sci.* **2022**, *119*, No. e2110867119.

(14) Nakanishi, J.; Kikuchi, Y.; Takarada, T.; Nakayama, H.; Yamaguchi, K.; Maeda, M. Photoactivation of a Substrate for Cell Adhesion under Standard Fluorescence Microscopes. *J. Am. Chem. Soc.* **2004**, *126*, 16314−16315.

(15) Petersen, S.; Alonso, J. M.; Specht, A.; Duodu, P.; Goeldner, M.; del Campo, A. Phototriggering of Cell Adhesion by Caged Cyclic RGD Peptides. *Angew. Chem.* **2008**, *120*, 3236−3239.

(16) Ohmuro-Matsuyama, Y.; Tatsu, Y. Photocontrolled Cell Adhesion on a Surface Functionalized with a Caged Arginine-Glycine-Aspartate Peptide. *Angew. Chem., Int. Ed.* **2008**, *47*, 7527−7529.

(17) Lee, T. T.; García, J. R.; Paez, J. I.; Singh, A.; Phelps, E. A.; Weis, S.; Shafiq, Z.; Shekaran, A.; del Campo, A.; García, A. J. Light-Triggered in Vivo Activation of Adhesive Peptides Regulates Cell Adhesion, Inflammation and Vascularization of Biomaterials. *Nat. Mater.* **2015**, *14*, 352−360.

(18) Yamahira, S.; Misawa, R.; Kosaka, T.; Tan, M.; Izuta, S.; Yamashita, H.; Heike, Y.; Okamoto, A.; Nagamune, T.; Yamaguchi, S. Photoactivatable Materials for Versatile Single-Cell Patterning Based on the Photocaging of Cell-Anchoring Moieties through Lipid Self-Assembly. *J. Am. Chem. Soc.* **2022**, *144*, 13154−13162.

(19) Poloukhtine, A. A.; Mbua, N. E.; Wolfert, M. A.; Boons, G.-J.; Popik, V. V. Selective Labeling of Living Cells by a Photo-Triggered Click Reaction. *J. Am. Chem. Soc.* **2009**, *131*, 15769−15776.

(20) Du, H.; Chandaroy, P.; Hui, S. W. Grafted Poly-(Ethylene Glycol) on Lipid Surfaces Inhibits Protein Adsorption and Cell Adhesion. *Biochim. Biophys. Acta, Biomembr.* **1997**, *1326*, 236−248.

(21) Teramura, Y.; Iwata, H. Cell Surface Modification with Polymers for Biomedical Studies. *Soft Matter* **2010**, *6*, 1081.

(22) Kato, K.; Umezawa, K.; Funeriu, D. P.; Miyake, M.; Miyake, J.; Nagamune, T. Immobilized Culture of Nonadherent Cells on an Oleyl Poly(Ethylene Glycol) Ether-Modified Surface. *BioTechniques* **2003**, *35*, 1014−1021.

(23) Takano, T.; Yamaguchi, S.; Matsunuma, E.; Komiya, S.; Shinkai, M.; Takezawa, T.; Nagamune, T. Cell Transfer Printing from Patterned Poly(Ethylene Glycol)-Oleyl Surfaces to Biological Hydrogels for

Rapid and Efficient Cell Micropatterning. *Biotechnol. Bioeng.* **2012**, *109*, 244−251.
(24) Yamaguchi, S.; Yamahira, S.; Kikuchi, K.; Sumaru, K.; Kanamori, T.; Nagamune, T. Photocontrollable Dynamic Micropatterning of Non-Adherent Mammalian Cells Using a Photocleavable Poly-(Ethylene Glycol) Lipid. *Angew. Chem., Int. Ed.* **2012**, *51*, 128−131.
(25) Yamahira, S.; Yamaguchi, S.; Kawahara, M.; Nagamune, T. Collagen Surfaces Modified with Photo-Cleavable Polyethylene Glycol-Lipid Support Versatile Single-Cell Arrays of Both Non-Adherent and Adherent Cells. *Macromol. Biosci.* **2014**, *14*, 1670−1676.
(26) Tateno, H.; Toyota, M.; Saito, S.; Onuma, Y.; Ito, Y.; Hiemori, K.; Fukumura, M.; Matsushima, A.; Nakanishi, M.; Ohnuma, K.; Akutsu, H.; Umezawa, A.; Horimoto, K.; Hirabayashi, J.; Asashima, M. Glycome Diagnosis of Human Induced Pluripotent Stem Cells Using Lectin Microarray. *J. Biol. Chem.* **2011**, *286*, 20345−20353.
(27) Lee, Y.-H.; Iijima, M.; Kado, Y.; Mizohata, E.; Inoue, T.; Sugiyama, A.; Doi, H.; Shibasaki, Y.; Kodama, T. Construction and Characterization of Functional Anti-Epiregulin Humanized Monoclonal Antibodies. *Biochem. Biophys. Res. Commun.* **2013**, *441*, 1011−1017.
(28) Baba, I.; Shirasawa, S.; Iwamoto, R.; Okumura, K.; Tsunoda, T.; Nishioka, M.; Fukuyama, K.; Yamamoto, K.; Mekada, E.; Sasazuki, T. Involvement of Deregulated Epiregulin Expression in Tumorigenesis in Vivo through Activated Ki-Ras Signaling Pathway in Human Colon Cancer Cells. *Cancer Res.* **2000**, *60*, 6886−6889.
(29) Hammer, Q.; Rückert, T.; Romagnani, C. Natural Killer Cell Specificity for Viral Infections. *Nat. Immunol.* **2018**, *19*, 800−808.
(30) Liu, X.; Li, L.; Si, F.; Huang, L.; Zhao, Y.; Zhang, C.; Hoft, D. F.; Peng, G. NK and NKT Cells Have Distinct Properties and Functions in Cancer. *Oncogene* **2021**, *40*, 4521−4537.
(31) Zheng, M.; Gao, Y.; Wang, G.; Song, G.; Liu, S.; Sun, D.; Xu, Y.; Tian, Z. Functional Exhaustion of Antiviral Lymphocytes in COVID-19 Patients. *Cell. Mol. Immunol.* **2020**, *17*, 533−535.
(32) Demaria, O.; Carvelli, J.; Batista, L.; Thibult, M.-L.; Morel, A.; André, P.; Morel, Y.; Vély, F.; Vivier, E. Identification of Druggable Inhibitory Immune Checkpoints on Natural Killer Cells in COVID-19. *Cell. Mol. Immunol.* **2020**, *17*, 995−997.
(33) Ullberg, M.; Jondal, M. Recycling and Target Binding Capacity of Human Natural Killer Cells. *J. Exp. Med.* **1981**, *153*, 615−628.
(34) Backes, C. S.; Friedmann, K. S.; Mang, S.; Knörck, A.; Hoth, M.; Kummerow, C. Natural Killer Cells Induce Distinct Modes of Cancer Cell Death: Discrimination, Quantification, and Modulation of Apoptosis, Necrosis, and Mixed Forms. *J. Biol. Chem.* **2018**, *293*, 16348−16363.
(35) Prager, I.; Liesche, C.; van Ooijen, H.; Urlaub, D.; Verron, Q.; Sandström, N.; Fasbender, F.; Claus, M.; Eils, R.; Beaudouin, J.; Önfelt, B.; Watzl, C. NK Cells Switch from Granzyme B to Death Receptor−Mediated Cytotoxicity during Serial Killing. *J. Exp. Med.* **2019**, *216*, 2113−2127.
(36) Owen-Schaub, L. B.; Zhang, W.; Cusack, J. C.; Angelo, L. S.; Santee, S. M.; Fujiwara, T.; Roth, J. A.; Deisseroth, A. B.; Zhang, W. W.; Kruzel, E. Wild-Type Human P53 and a Temperature-Sensitive Mutant Induce Fas/APO-1 Expression. *Mol. Cell. Biol.* **1995**, *15*, 3032−3040.
(37) Friscourt, F.; Ledin, P. A.; Mbua, N. E.; Flanagan-Steet, H. R.; Wolfert, M. A.; Steet, R.; Boons, G.-J. Polar Dibenzocyclooctynes for Selective Labeling of Extracellular Glycoconjugates of Living Cells. *J. Am. Chem. Soc.* **2012**, *134*, 5381−5389.

https://doi.org/10.1021/jacs.2c07321
J. Am. Chem. Soc. XXXX, XXX, XXX−XXX